Electronic Supplementary Material (ESI) for Dalton Transactions.

Macrocycle Based Dinuclear Dysprosium(III) Single Molecule Magnets with Local D_{5h} Coordination Geometry

Jianfeng Wu,[a,b] Serhiy Demeshko,[a] Sebastian Dechert,[a] and Franc Meyer*,[a]

[a] Institut für Anorganische Chemie, Universität Göttingen, Tammannstr. 4, D-37077 Göttingen, Germany.

[b] School of Chemistry and Chemical Engineering, Northwestern Polytechnical University, Xi'an 710072, P. R. China

1. Schematic drawing of the ligands

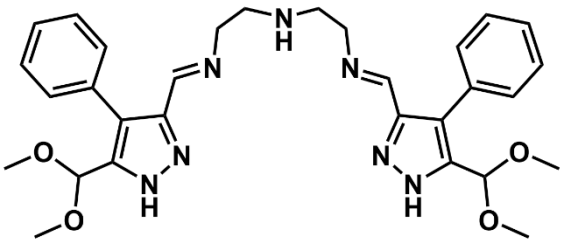

H_2L^1

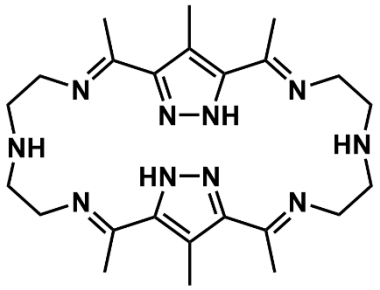

H_2L^2

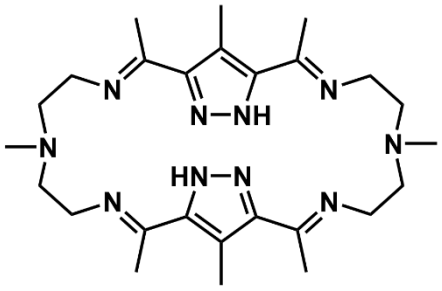

H_2L^3

Scheme S1. Schematic drawing of the proligands H_2L^1 (top), H_2L^2 (middle), and H_2L^3 (bottom).

2. IR Spectroscopy

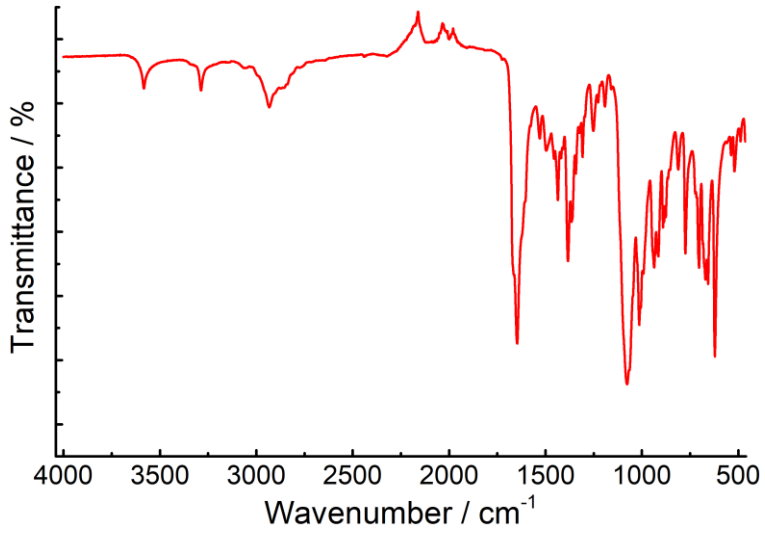

Fig. S1 IR(ATR) spectrum of a solid sample of complex **Dy4**.

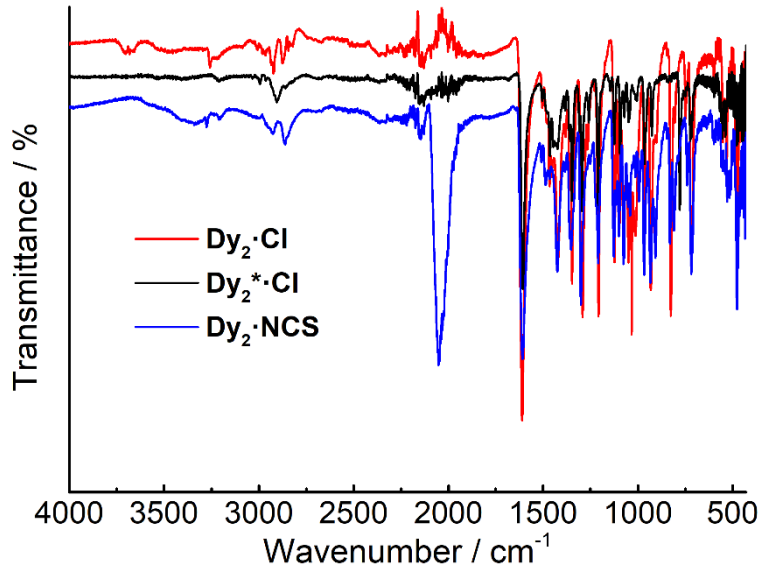

Fig. S2 IR(ATR) spectra of solid samples of complexes **Dy2·Cl**, **Dy2*·Cl**, and **Dy2·SCN**.

3. Powder XRD and thermogravimetric analyses

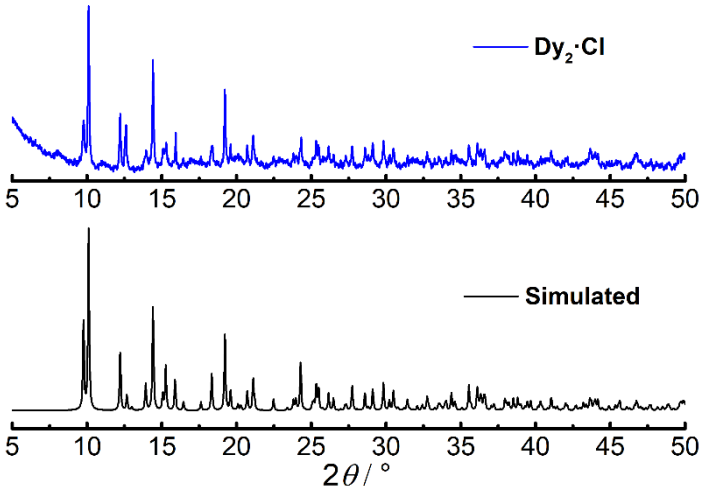

Fig. S3 Powder XRD analysis of **Dy_2·Cl**. The black line is the simulated pattern based on the single crystal diffraction data.

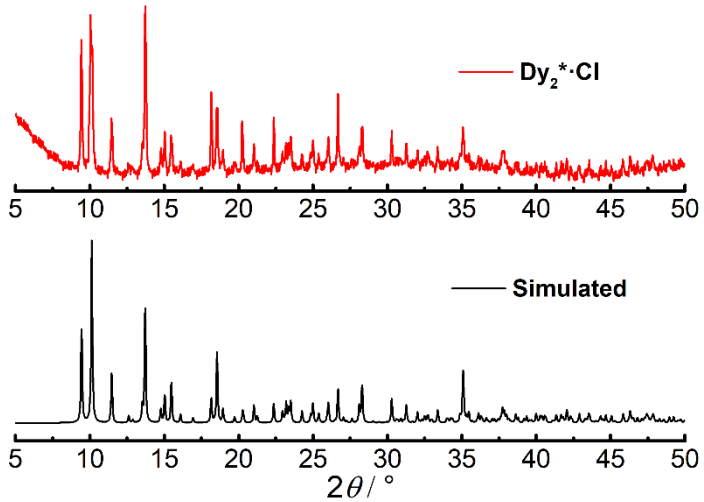

Fig. S4 Powder XRD analysis of **Dy_2^*·Cl**. The black line is the simulated pattern based on the single crystal diffraction data.

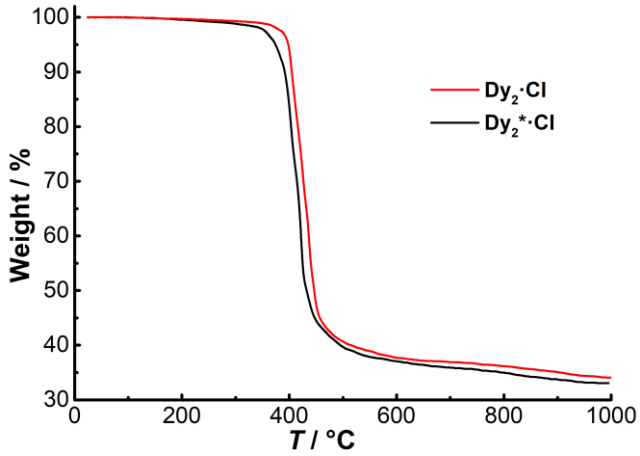

Fig. S5 Thermogravimetric analyses of **Dy_2·Cl** (red line) and **Dy_2^*·Cl** (black line).

4. Crystallographic Details

Table S1. Crystallographic data of complexes **Dy_4**, **Dy_2·Cl**, **Dy_2^*·Cl**, and **Dy_2·SCN**.

	Dy_4	**Dy_2·Cl**	**Dy_2^*·Cl**	**Dy_2·SCN**
empirical formula	$C_{72}H_{102}Cl_4Dy_4N_{18}O_{32}$	$C_{24}H_{36}Cl_4Dy_2N_{10}$	$C_{26}H_{40}Cl_4Dy_2N_{10}$	$C_{30}H_{44}Dy_2N_{14}O_2S_4$
formula weight, g·mol^{-1}	2523.51	931.43	959.48	1086.03
crystal size, mm³	0.500 x 0.300 x 0.150	0.210 x 0.180 x 0.160	0.160 x 0.150 x 0.100	0.210 x 0.080 x 0.050
crystal system	Monoclinic	Monoclinic	Monoclinic	Triclinic
space group	$P2_1/n$	$P2_1/c$	$P2_1/c$	P-1
T, K	133(2)	133(2)	133(2)	133(2)
λ, Å	0.71073	0.71073	0.71073	0.71073
a, Å	14.0320(2)	8.9982(3)	8.9524(3)	8.7415(4)
b, Å	16.1940(3)	11.6001(3)	11.7805(5)	9.1291(4)
c, Å	25.7815(4)	14.8941(5)	15.8173(6)	12.9791(5)
α, °	90	90	90	79.287(3)
β, °	96.4540(10)	103.545(3)	102.837(3)	73.578(3)
γ, °	90	90	90	87.499(4)
V, Å^3	5821.31(16)	1511.41(8)	1626.46(11)	976.15(7)
Z	2	2	2	1
ρ (cal), g·cm^{-3}	1.440	2.047	1.959	1.847
F(000)	2496	900	932	534
θ range [°]	1.488 to 26.790	2.250 to 26.855	2.175 to 26.865	1.663 to 26.747
Tmin / Tmax	0.8436 / 0.5310	0.4310 / 0.2492	0.8004 / 0.6557	0.8473 / 0.4952
measured refl.	84214	19848	13782	13784
unique refl. [Rint]	12347, 0.0285	3205 / 0.0239	3450 / 0.0360	4139 / 0.0275
goodness-of-fit (F^2)	1.048	1.115	1.071	1.118
data / restr. / param.	12347 / 119 / 636	3205 / 0 / 184	3450 / 31 / 241	4139 / 1 / 247
$R1$, $wR2$ ($I > 2\sigma(I)$)	0.0235, 0.0569	0.0248, 0.0589	0.0293, 0.0638	0.0229, 0.0537
$R1$, $wR2$ (all data)	0.0274, 0.0584	0.0275, 0.0600	0.0400, 0.0668	0.0282, 0.0558
res. el. dens. [e·Å^{-3}]	0.736 / -0.686	1.257 / -0.717	1.882 / -0.700	1.492 / -0.336

Table S2. Selected bond distances (Å) in complex **Dy_4**.

Dy(1)-O(6)	2.2608(18)	Dy(2)-O(6)	2.2726(19)
Dy(1)-O(5)	2.3152(18)	Dy(2)-O(8)	2.320(2)
Dy(1)-O(7)	2.351(2)	Dy(2)-O(5)	2.3890(18)
Dy(1)-O(5)#	2.4034(17)	Dy(2)-N(6)#	2.411(2)
Dy(1)-N(1)	2.424(2)	Dy(2)-N(2)#	2.431(2)
Dy(1)-N(7)	2.429(2)	Dy(2)-N(3)#	2.517(2)
Dy(1)-O(1)	2.5179(19)	Dy(2)-N(5)#	2.531(2)
Dy(1)-O(3)	2.5892(19)	Dy(2)-N(4)#	2.570(2)
Dy(1)-Dy(1)#	3.8066(2)	Dy(1)-Dy(2)	3.72071(18)

Symmetry transformations used to generate equivalent atoms: # -x+1,-y+1,-z+1.

Table S3. Selected bond angles (°) in complex **Dy_4**.

O(6)-Dy(1)-O(7)	82.39(7)	O(6)-Dy(2)-O(8)	98.08(8)
O(5)-Dy(1)-O(7)	105.47(7)	O(8)-Dy(2)-O(5)	82.54(7)
O(7)-Dy(1)-N(1)	78.31(8)	O(6)-Dy(2)-N(6)#	86.75(7)
O(5)#-Dy(1)-N(1)	74.10(7)	O(5)-Dy(2)-N(6)#	73.90(7)
O(5)-Dy(1)-N(7)	80.54(7)	O(8)-Dy(2)-N(2)#	85.35(8)
O(5)#-Dy(1)-N(7)	75.54(7)	N(6)#-Dy(2)-N(2)#	75.44(8)
N(1)-Dy(1)-N(7)	75.15(8)	O(8)-Dy(2)-N(3)#	82.04(8)
O(6)-Dy(1)-O(1)	85.28(7)	N(6)#-Dy(2)-N(3)#	105.55(8)
O(7)-Dy(1)-O(1)	86.00(7)	O(6)-Dy(2)-N(5)#	84.66(7)
N(7)-Dy(1)-O(1)	105.67(7)	N(2)#-Dy(2)-N(5)#	114.67(8)
O(6)-Dy(1)-O(3)	78.91(7)	N(3)#-Dy(2)-N(5)#	79.15(8)
O(5)-Dy(1)-O(3)	82.41(6)	O(6)-Dy(2)-N(4)#	86.46(7)
N(1)-Dy(1)-O(3)	109.12(7)	O(8)-Dy(2)-N(4)#	76.38(8)
O(1)-Dy(1)-O(3)	78.54(7)	N(2)#-Dy(2)-N(4)#	129.56(8)

Symmetry transformations used to generate equivalent atoms: # -x+1,-y+1,-z+1

Table S4. Selected bond distances (Å) and angles (°) in complexes **Dy_2·Cl**, **Dy_2^*·Cl**, and **Dy_2·SCN**.

Dy_2·Cl		**Dy_2^*·Cl**		**Dy_2·SCN**	
Dy(1)-N(1)	2.441(3)	Dy(1)-N(5)	2.447(4)	Dy(1)-N(6)	2.397(3)
Dy(1)-N(2)	2.455(3)	Dy(1)-N(2)	2.452(3)	Dy(1)-N(7)	2.423(3)
Dy(1)-N(5)	2.458(3)	Dy(1)-N(1)	2.453(4)	Dy(1)-N(1)	2.454(3)
Dy(1)-N(3)	2.467(3)	Dy(1)-N(3)	2.469(4)	Dy(1)-O(1)	2.455(3)
Dy(1)-N(4)	2.488(4)	Dy(1)-N(4)	2.547(4)	Dy(1)-N(2)	2.472(3)
Dy(1)-Cl(2)	2.6030(11)	Dy(1)-Cl(2)	2.6050(12)	Dy(1)-N(3)	2.484(3)
Dy(1)-Cl(1)	2.6143(12)	Dy(1)-Cl(1)	2.6123(12)	Dy(1)-N(5)	2.486(3)
Cl(2)-Dy(1)-Cl(1)	169.18(4)	Cl(2)-Dy(1)-Cl(1)	174.17(4)	Dy(1)-N(4)	2.550(3)
				N(6)-Dy(1)-N(7)	149.49(10)
				N(7)-Dy(1)-O(1)	138.69(9)

Table S5. Selected bond angles (°) in complexes **Dy_2·Cl**, **Dy_2^*·Cl**, and **Dy_2·SCN**.

Dy_2·Cl		**Dy_2^*·Cl**		**Dy_2·SCN**	
N(1)-Dy(1)-N(2)	92.58(10)	N(5)-Dy(1)-N(2)	66.32(13)	N(6)-Dy(1)-N(1)	112.19(10)
N(2)-Dy(1)-N(5)	66.02(11)	N(2)-Dy(1)-N(1)	91.34(11)	N(7)-Dy(1)-N(1)	81.24(9)
N(1)-Dy(1)-N(3)	66.12(11)	N(1)-Dy(1)-N(3)	66.33(12)	N(6)-Dy(1)-O(1)	71.50(9)
N(5)-Dy(1)-N(4)	68.46(13)	N(5)-Dy(1)-N(4)	67.26(13)	N(6)-Dy(1)-N(2)	127.67(10)
N(3)-Dy(1)-N(4)	66.81(13)	N(3)-Dy(1)-N(4)	68.76(13)	N(7)-Dy(1)-N(2)	76.78(9)
N(1)-Dy(1)-Cl(2)	92.58(8)	N(5)-Dy(1)-Cl(2)	90.98(13)	N(1)-Dy(1)-N(2)	91.53(9)
N(2)-Dy(1)-Cl(2)	94.97(8)	N(2)-Dy(1)-Cl(2)	93.43(8)	N(6)-Dy(1)-N(3)	80.86(10)
N(5)-Dy(1)-Cl(2)	90.78(9)	N(1)-Dy(1)-Cl(2)	89.92(9)	N(7)-Dy(1)-N(3)	80.60(10)
N(3)-Dy(1)-Cl(2)	88.08(8)	N(3)-Dy(1)-Cl(2)	86.31(9)	N(1)-Dy(1)-N(3)	65.20(9)
N(4)-Dy(1)-Cl(2)	85.43(12)	N(4)-Dy(1)-Cl(2)	88.08(9)	N(6)-Dy(1)-N(5)	90.11(10)
N(1)-Dy(1)-Cl(1)	93.73(8)	N(5)-Dy(1)-Cl(1)	90.22(13)	N(7)-Dy(1)-N(5)	84.64(10)
N(2)-Dy(1)-Cl(1)	93.53(8)	N(2)-Dy(1)-Cl(1)	92.28(8)	N(2)-Dy(1)-N(5)	65.31(9)

N(5)-Dy(1)-Cl(1)	86.55(9)	N(1)-Dy(1)-Cl(1)	91.14(9)	N(6)-Dy(1)-N(4)	70.54(10)
N(3)-Dy(1)-Cl(1)	86.45(9)	N(3)-Dy(1)-Cl(1)	88.86(9)	N(7)-Dy(1)-N(4)	79.86(10)
N(4)-Dy(1)-Cl(1)	83.83(12)	N(4)-Dy(1)-Cl(1)	87.12(9)	N(3)-Dy(1)-N(4)	66.24(9)
				N(5)-Dy(1)-N(4)	66.46(9)

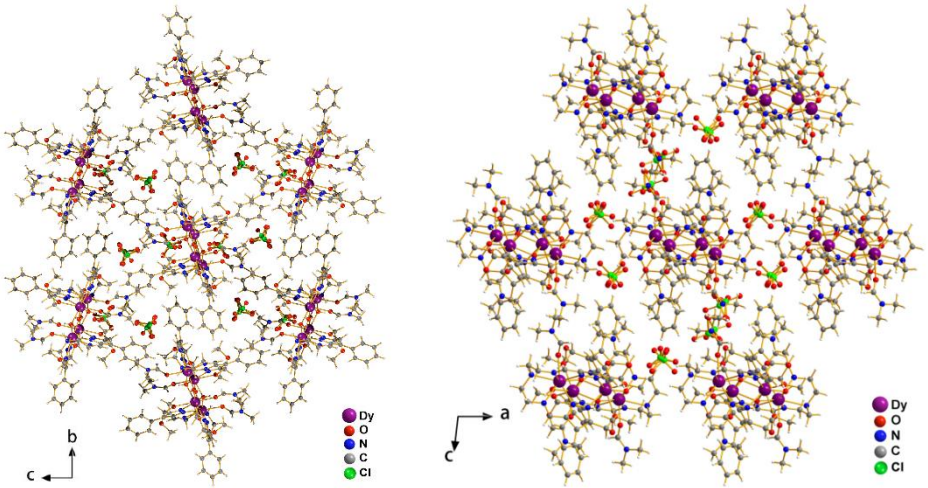

Fig. S6 Packing models along the *a* and *b* axes of complex **Dy$_4$**.

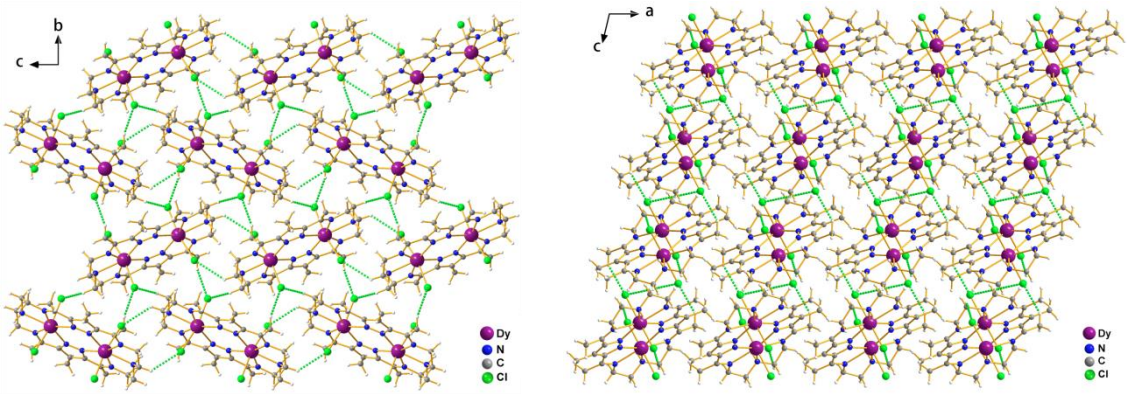

Fig. S7 Packing models along the *a* and *b* axes of complex **Dy$_2$·Cl**. The green dash lines represent the hydrogen bondings.

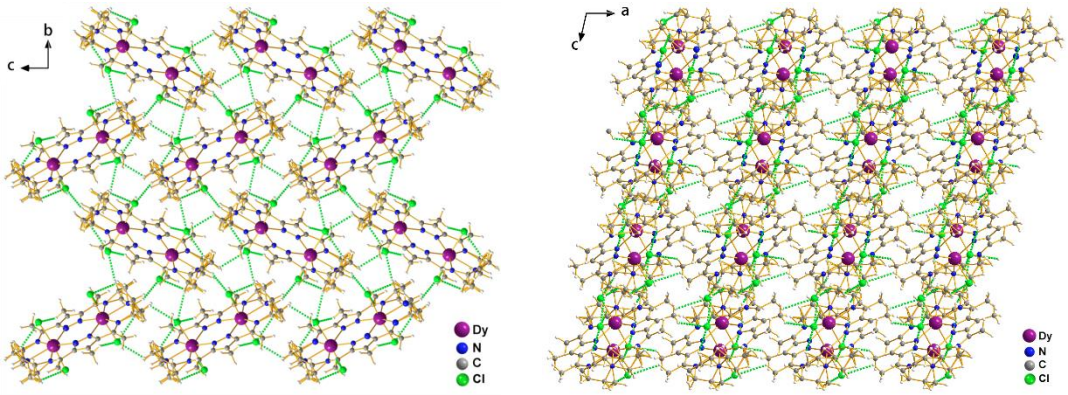

Fig. S8 Packing models along the *a* and *b* axes of complex **Dy$_2$*·Cl**. The green dash lines represent the hydrogen bondings.

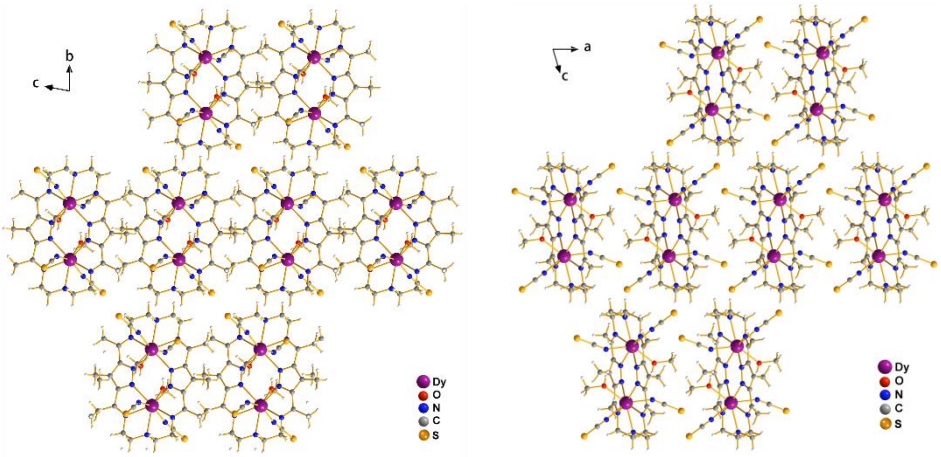

Fig. S9 Packing models along the *a* and *b* axes of complex **Dy_2·SCN**.

Table S6. *CShM* values calculated by *SHAPE* 2.1[1] for **Dy_4**.

Central atom	Coordination Geometry	Dy1	Dy2
Dy	Cube (O_h)	10.878	12.616
	Square antiprism (D_{4d})	**1.358**	2.900
	Triangular dodecahedron (D_{2d})	2.124	2.075
	Johnson gyrobifastigium J26 (D_{2d})	15.159	11.704
	Johnson elongated triangular bipyramid (D_{3h})	28.301	25.449
	Biaugmented trigonal prism (C_{2v})	2.147	**1.898**
	Snub diphenoid J84 (D_{2d})	4.694	3.447

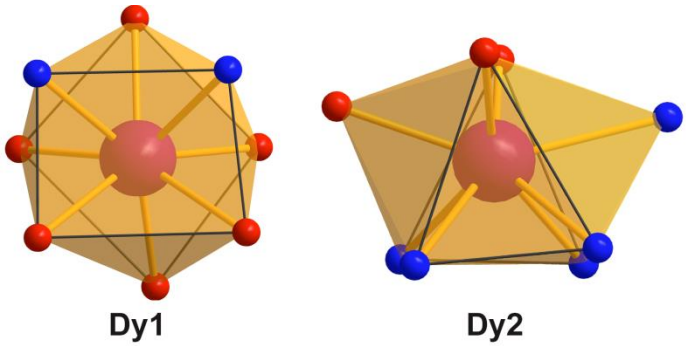

Fig. S10 Coordination polyhedron of Dy1 (left) and Dy2 (right) in complex **Dy_4**.

Table S7. *CShM* values calculated by *SHAPE* 2.1[1] for **Dy_2·Cl** and **Dy_2^*·Cl**.

Central atom	Coordination Geometry	**Dy_2·Cl**	**Dy_2^*·Cl**
Dy	Hexagonal pyramid (C_{6v})	24.940	24.584
	Pentagonal bipyramid (D_{5h})	**0.801**	**0.689**
	Capped octahedron (C_{3v})	8.759	8.143
	Capped trigonal prism (C_{2v})	6.947	6.420
	Johnson pentagonal bipyramid J13 (D_{5h})	5.420	5.268
	Johnson elongated triangular pyramid J7 (C_{3v})	24.391	23.565

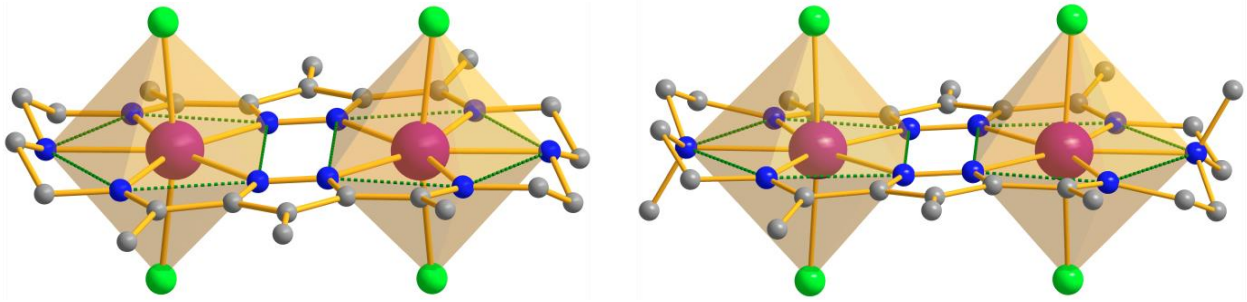

Fig. S11 Coordination polyhedra of the Dy^{III} ions in complexes **Dy_2·Cl** (left) and **Dy_2^*·Cl** (right).

Table S8. *CShM* values calculated by *SHAPE* 2.1[1] for **Dy_2·SCN**.

Central atom	Coordination Geometry	**Dy_2·SCN**
Dy	Cube (O_h)	8.776
	Square antiprism (D_{4d})	4.194
	Triangular dodecahedron (D_{2d})	**2.600**
	Johnson gyrobifastigium J26 (D_{2d})	9.308
	Johnson elongated triangular bipyramid (D_{3h})	26.603
	Biaugmented trigonal prism (C_{2v})	2.818
	Snub diphenoid J84 (D_{2d})	5.724

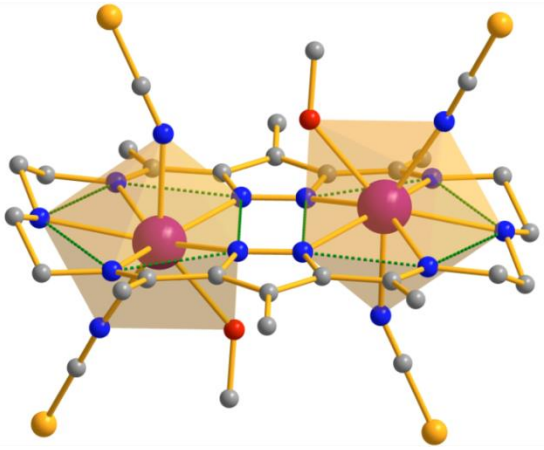

Fig. S12 Coordination polyhedra of the Dy^{III} ions in complex **Dy_2·SCN**.

5. Direct current (dc) magnetic susceptibility measurements

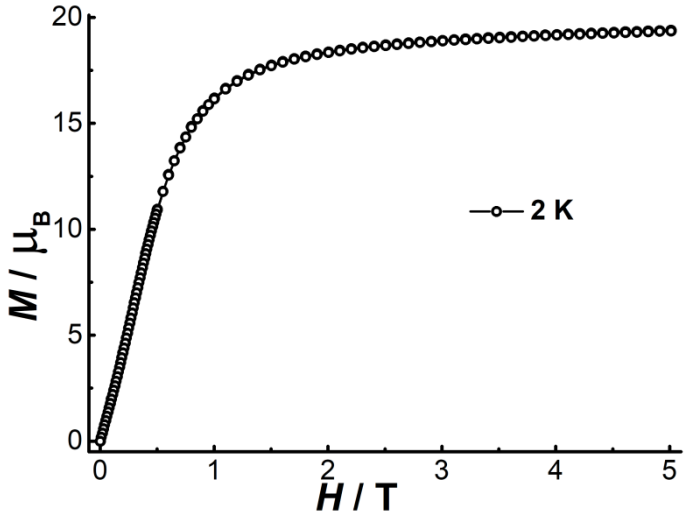

Fig. S13 Molar magnetization (*M*) *vs*. field (*H*) for **Dy$_4$** at 2.0 K.

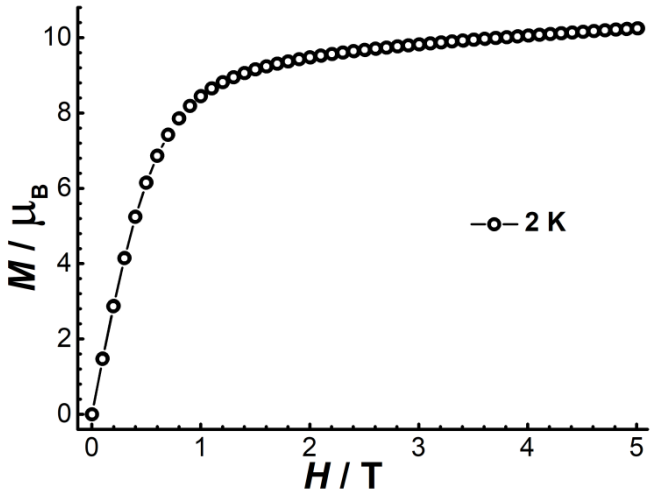

Fig. S14 Molar magnetization (*M*) *vs*. field (*H*) for **Dy$_2$·Cl** at 2.0 K.

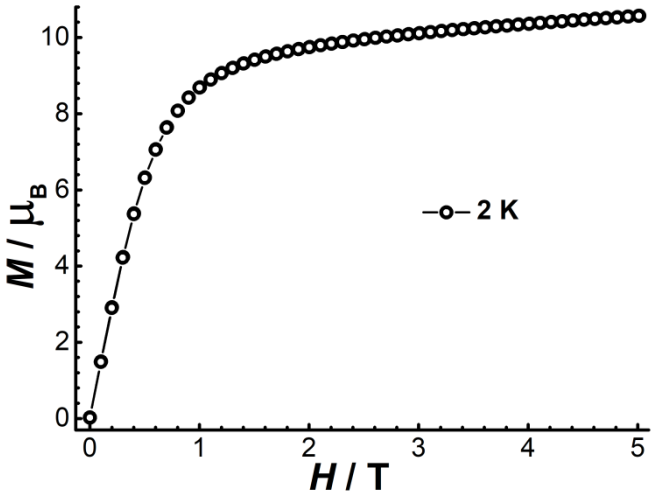

Fig. S15 Molar magnetization (*M*) *vs*. field (*H*) for **Dy_2*·Cl** at 2.0 K.

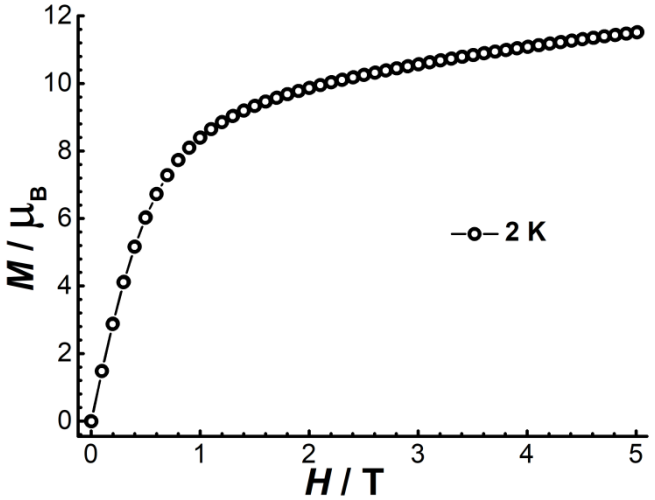

Fig. S16 Molar magnetization (*M*) *vs*. field (*H*) for **Dy_2·SCN** at 2.0 K.

6. Alternating current (ac) magnetic susceptibility measurements

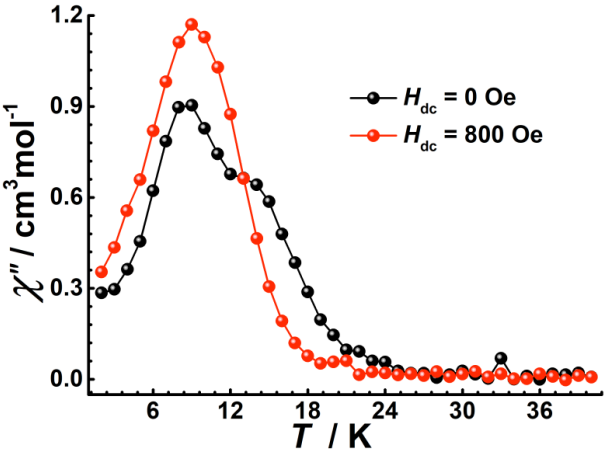

Fig. S17 Temperature-dependent ac susceptibility of **Dy$_4$** at indicated dc fields with frequency of 1488 Hz.

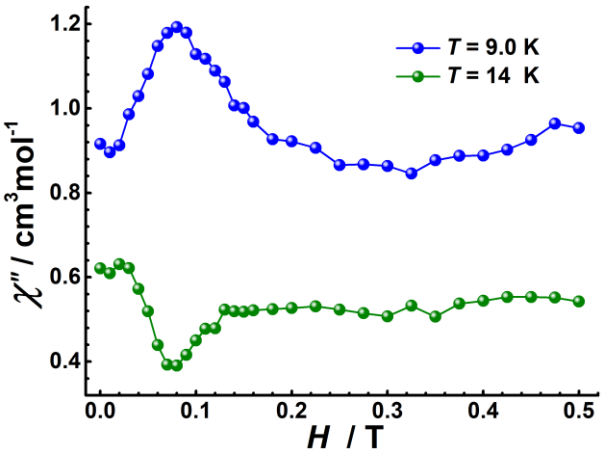

Fig. S18 Field-dependent ac susceptibility of **Dy$_4$** at indicated temperatures with frequency of 1488 Hz.

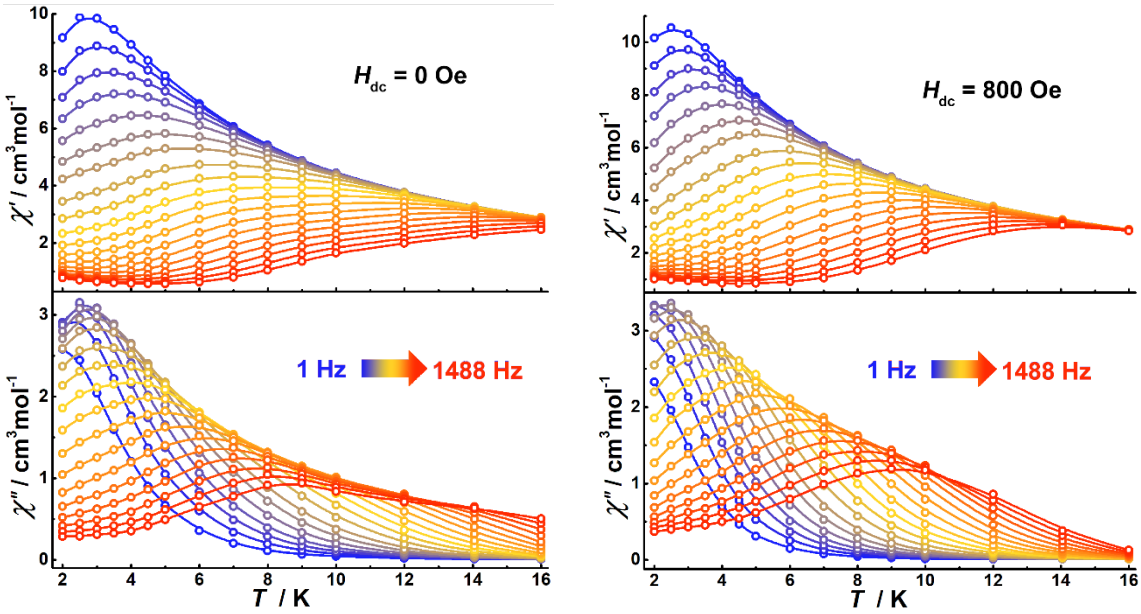

Fig. S19 Temperature-dependent ac susceptibility of **Dy_4** at indicated frequencies under zero (left) and 800 Oe (right) dc field.

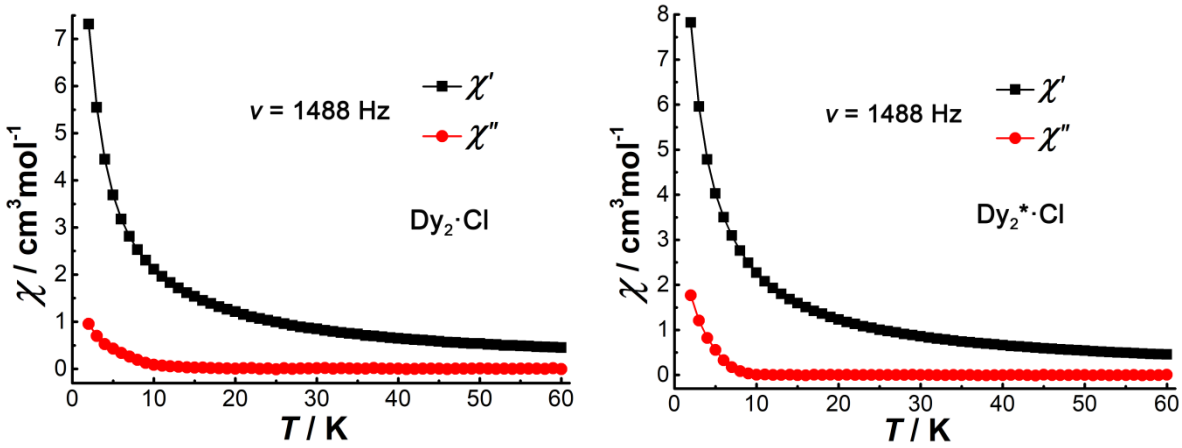

Fig. S20 Temperature-dependent ac susceptibility of **Dy_2·Cl** (left) and **Dy_2^*·Cl** (right) at zero dc field with a frequency of 1488 Hz.

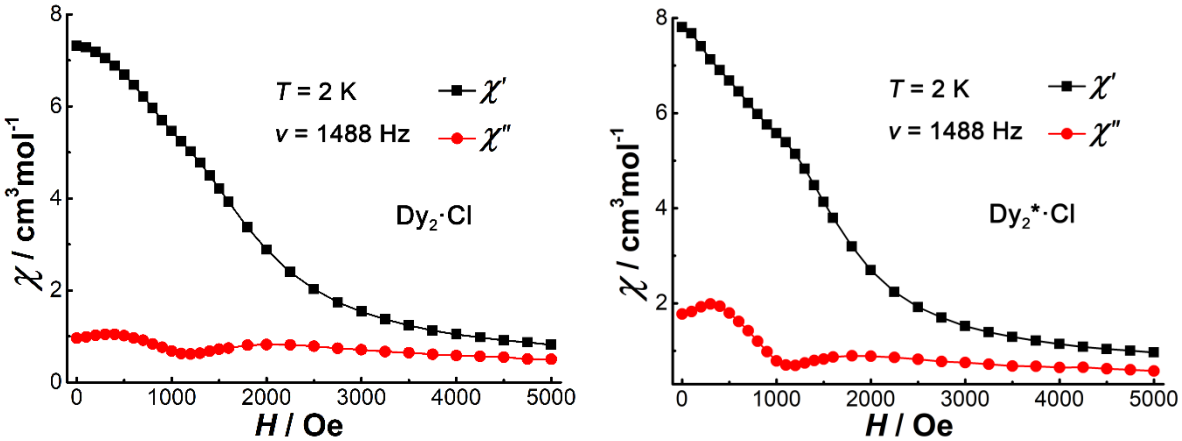

Fig. S21 Field-dependent ac susceptibility of **Dy_2·Cl** (left) and **Dy_2^*·Cl** (right) at 2 K with a frequency of 1488 Hz.

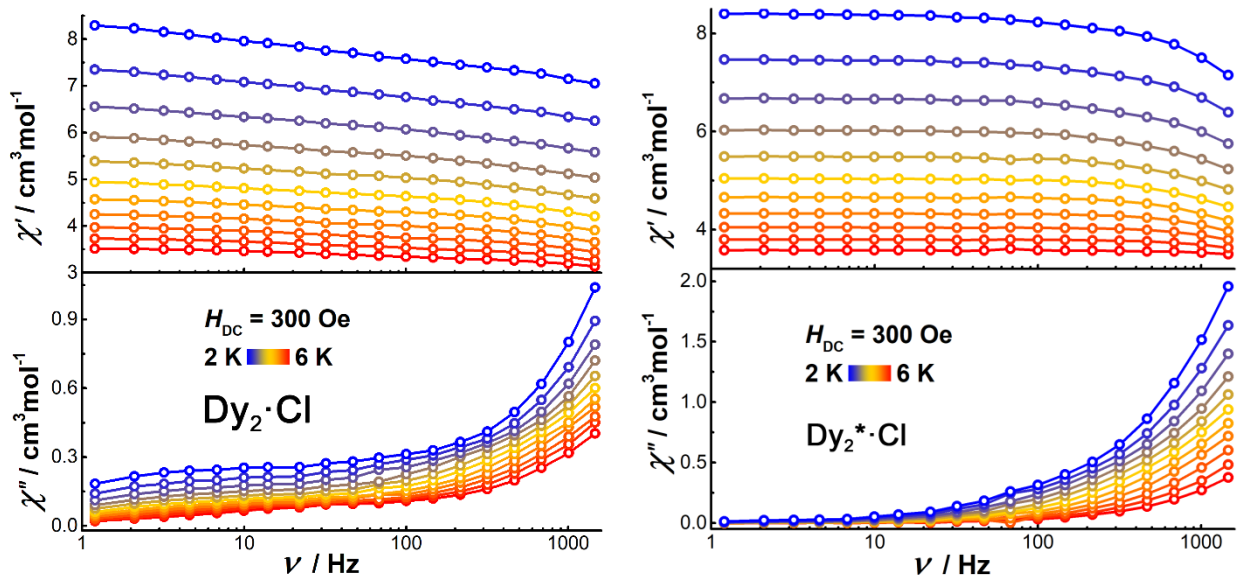

Fig. S22 Frequency-dependent ac susceptibility of **Dy_2·Cl** (left) and **Dy_2^*·Cl** (right) at indicated temperatures under 300 Oe dc field.

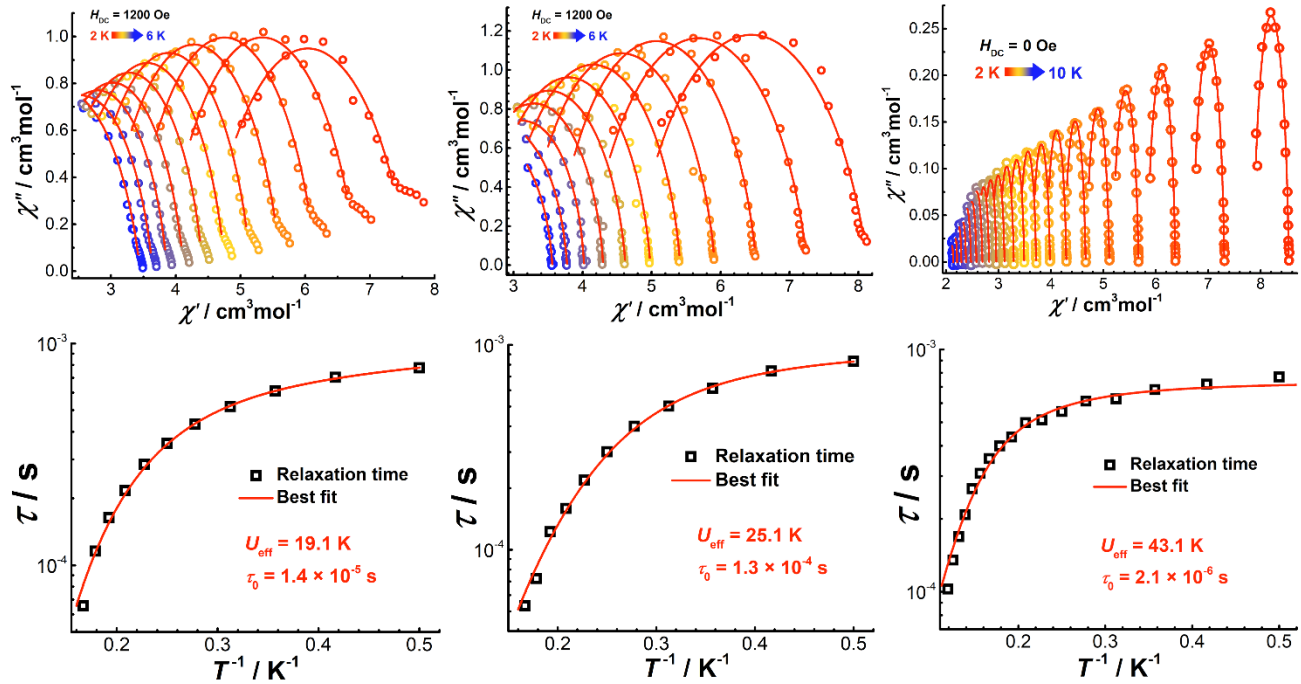

Fig. S23 Cole-Cole plots (top) and plots of τ *vs.* T^{-1} (bottom) for **Dy_2·Cl** (left), **Dy_2^*·Cl** (middle), and **Dy_2·SCN** (right) under indicated dc field. The red line represents the best fits using equation 1.

7. CC-Fit results

Table S9. CC-Fit[2] results for frequency-dependent ac susceptibility of **Dy_4** under zero dc field.

T / K	$\chi_{S,tot}$	$\Delta\chi_1$	τ_1 / s	α_1	$\Delta\chi_2$	τ_2 / s	α_2	*Residual*
2	0.59044	8.13929	0.01481	0.32966	2.64099	0.09655	2.19926E-8	0.01591
2.5	0.5123	8.08732	0.01224	0.31826	2.93527	0.07771	3.18221E-8	0.00888
3	0.4305	8.05426	0.01076	0.32373	2.59776	0.05837	5.76599E-8	0.00764
3.5	0.37351	7.74295	0.00872	0.32463	2.23654	0.04503	1.18424E-7	0.00712
4	0.32768	7.29461	0.0066	0.32239	1.93835	0.03572	1.94098E-7	0.00725
4.5	0.274	6.84936	0.00482	0.32419	1.70276	0.02866	3.94594E-7	0.00647
5	0.22708	6.386	0.00344	0.32719	1.5474	0.02289	7.95211E-7	0.00522
6	0.13659	5.53512	0.00171	0.33536	1.37677	0.01423	1.36364E-6	0.00559
7	0.11242	4.80641	9.03371E-4	0.34297	1.2644	0.00879	1.63469E-6	0.0059
8	0.07596	4.23591	4.81184E-4	0.36112	1.1917	0.00533	2.83498E-6	0.00695
9	0.15701	3.64447	2.70302E-4	0.37318	1.14825	0.00328	2.66936E-6	0.00912
10	0.5111	2.92288	1.98751E-4	0.35343	1.05345	0.00212	1.89458E-5	0.00817
12	0.99713	1.94597	1.11583E-4	0.28187	0.84326	8.84435E-4	2.65224E-5	0.00364
14	0.90483	1.72157	3.72505E-5	0.24227	0.64899	3.7311E-4	9.21447E-7	0.00178
16	0.97553	1.52834	2.23824E-5	0.14896	0.39461	1.83002E-4	1.00345E-6	0.00139

Table S10. CC-Fit results for frequency-dependent ac susceptibility of **Dy_4** under 800 Oe dc field.

T / K	χ_S	χ_T	τ / s	α	*Residual*
2	0.899	12.6174	0.02894	0.34231	0.07056
2.5	0.83	12.4717	0.02089	0.33558	0.09002
3	0.76931	11.6902	0.01471	0.32453	0.12673
3.5	0.72041	10.7396	0.01018	0.31072	0.15109
4	0.66365	9.8181	0.00696	0.29754	0.16413
4.5	0.61313	8.99414	0.00478	0.28615	0.15874
5	0.57009	8.2771	0.00332	0.27714	0.15522
6	0.50603	7.11298	0.0017	0.26438	0.1403
7	0.49822	6.21768	9.39959E-4	0.25406	0.11875
8	0.59089	5.51423	5.58594E-4	0.24155	0.09559
9	0.77069	4.94512	3.47387E-4	0.22478	0.06007
10	1.00678	4.48003	2.18822E-4	0.20507	0.03133
12	1.55972	3.77789	9.01896E-5	0.15865	0.00468

Table S11. Parameters obtained from the fitting of the relaxation time (τ) *vs.* 1/T plots of **Dy_4** under zero and 800 Oe dc field.

dc Field		U_{eff} / K	τ_0 / s	τ_{QTM} / s	AH^4	C	n
0 Oe	SR	59.21	9.26632E-6	0.10666	0	0.29684	3
	FR	48.66	1.08391E-5	0.01414	0	0.16781	4.44712
800 Oe		46.01	1.20876E-5	0.10134	9.41073	0.36298	4.01693

Table S12. CC-Fit results for frequency-dependent ac susceptibility of **Dy_2·Cl** under 1200 Oe dc field.

T / K	χ_S	χ_T	τ / s	α	*Residual*
6	1.1397	3.44922	6.5531E-5	0.27193	0.00726
5.6	1.54109	3.64313	1.15704E-4	0.22785	0.00742
5.2	1.74555	3.86974	1.64343E-4	0.21238	0.00743
4.8	1.93081	4.12384	2.17445E-4	0.20528	0.00667
4.4	2.15013	4.42094	2.84882E-4	0.19433	0.0069
4	2.36507	4.7635	3.53657E-4	0.19766	0.00723
3.6	2.63061	5.16303	4.31948E-4	0.2013	0.01003
3.2	2.94591	5.62515	5.19721E-4	0.21235	0.01019
2.8	3.33487	6.18075	6.09794E-4	0.23033	0.01758
2.4	3.86546	6.81802	7.03546E-4	0.25244	0.01993
2	4.47729	7.61702	7.76157E-4	0.31706	0.03457

Table S13. CC-Fit results for frequency-dependent ac susceptibility of **Dy_2*·Cl** under 1200 Oe dc field.

T / K	χ_S	χ_T	τ / s	α	*Residual*
6	2.13221	3.5558	5.31887E-5	0.11228	0.00408
5.6	2.09976	3.77139	7.23319E-5	0.12661	0.00344
5.2	2.32506	4.01674	1.22483E-4	0.08761	0.01621
4.8	2.30376	4.29555	1.59001E-4	0.11594	0.00702
4.4	2.40194	4.61804	2.18446E-4	0.13551	0.01218
4	2.61389	4.97832	3.00672E-4	0.13002	0.02068
3.6	2.88533	5.41094	4.00273E-4	0.13047	0.02073
3.2	3.19282	5.91298	5.01834E-4	0.1421	0.04243
2.8	3.61486	6.51272	6.15237E-4	0.14721	0.05933
2.4	4.10006	7.25575	7.44169E-4	0.19283	0.06518
2	4.75651	8.12786	8.31683E-4	0.22474	0.10165

Table S14. CC-Fit results for frequency-dependent ac susceptibility of **Dy_2·SCN** under zero dc field.

T / K	χ_S	χ_T	τ / s	α	*Residual*
2	7.86539	8.5371	7.70218E-4	0.14204	0.00285
2.4	6.71108	7.30889	7.1906E-4	0.14849	0.00176
2.8	5.84562	6.37441	6.82227E-4	0.14875	0.00103
3.2	5.18467	5.67092	6.25023E-4	0.16672	8.58981E-4
3.6	4.67764	5.11506	6.11415E-4	0.17049	7.4554E-4
4	4.26489	4.66411	5.54544E-4	0.16664	7.58629E-4
4.4	3.92149	4.29602	5.11631E-4	0.16921	7.95825E-4
4.8	3.65469	3.98292	4.98617E-4	0.15572	5.50063E-4
5.2	3.40823	3.71984	4.34641E-4	0.16145	4.80032E-4
5.6	3.20394	3.49263	3.99466E-4	0.16245	2.40736E-4
6	3.02766	3.29277	3.54213E-4	0.15223	2.10716E-4
6.4	2.87414	3.11717	3.08067E-4	0.1598	3.14756E-4
6.8	2.74039	2.96045	2.66174E-4	0.12979	2.72768E-4
7.2	2.6145	2.82158	2.0796E-4	0.14973	1.8885E-4
7.6	2.48542	2.69619	1.68795E-4	0.19989	1.79973E-4
8	2.41214	2.58167	1.35009E-4	0.162	1.8817E-4
8.4	2.3207	2.47823	1.02639E-4	0.19051	2.40235E-4

Table S15. Parameters obtained from the fitting of the relaxation time (τ) *vs.* 1/*T* plots of **Dy_2·Cl**, **Dy_2^*·Cl**, and **Dy_2·SCN**.

	U_{eff} / K	τ_0 / s	τ_{QTM} / s	AH^4	C	n
Dy_2·Cl	19.08	1.37486E-5	1.57E-3	321.65034	0.00849	7.57941
Dy_2^*·Cl	25.06	1.30265E-4	1.12E-3	121.91791	2.49935	4.83978
Dy_2·SCN	43.1	2.11156E-6	7.34E-4	0	5.11551	3.07443

8. Calculations with Magellan program

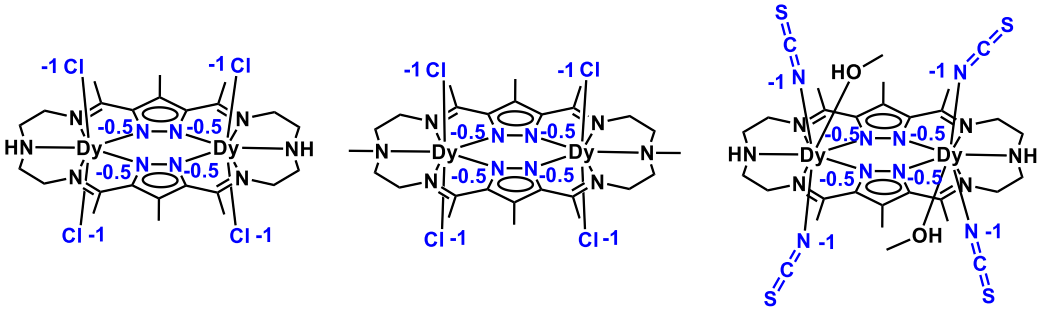

Fig. S24 Partial charges assigned to the ligands in complexes **Dy₂·Cl** (left), **Dy₂*·Cl** (middle), and **Dy₂·SCN** (right) with one negative charge in axial directions.

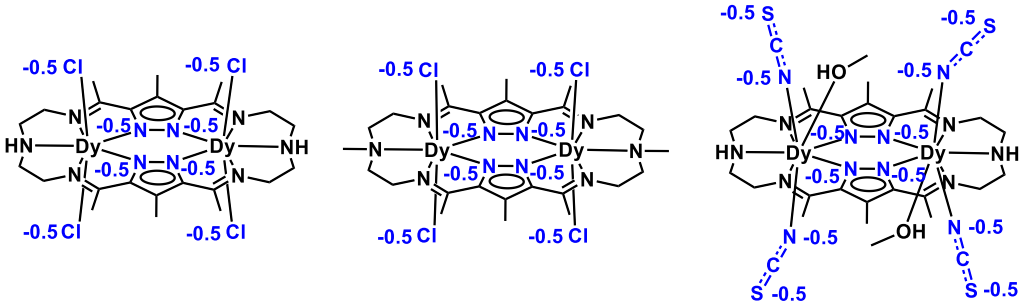

Fig. S25 Partial charges assigned to the ligands in complexes **Dy₂·Cl** (left), **Dy₂*·Cl** (middle), and **Dy₂·SCN** (right) with half negative charge in axial directions.

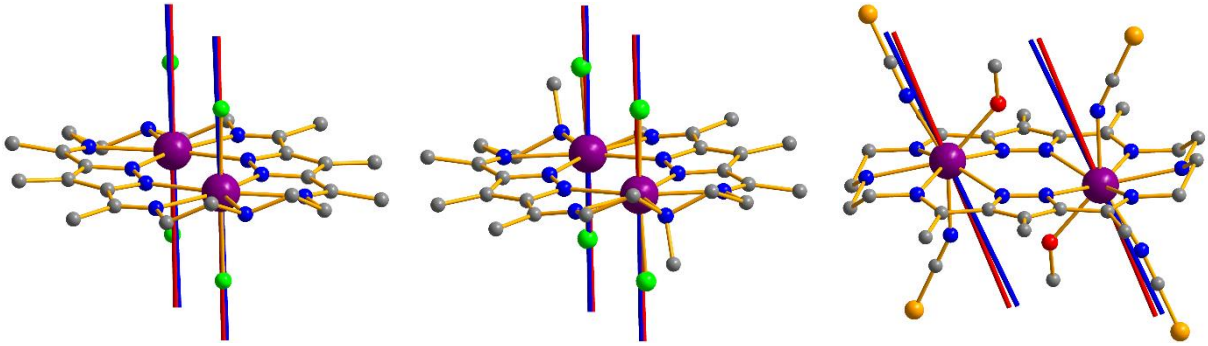

Fig. S26 Orientations of the main magnetic axes and local magnetizations of the ground states for the one (red) and half (blue) negative charge models of the **Dy₂·Cl** (left), **Dy₂*·Cl** (middle), and **Dy₂·NCS** (right).

Table S16. Minimal reorientation energies (cm^{-1}) and intersection angles (°) of anisotropy axes calculated from two different models by Magellan program[3] for complexes **Dy₂·Cl**, **Dy₂*·Cl**, and **Dy₂·SCN**.

	Dy₂·Cl		**Dy₂*·Cl**		**Dy₂·SCN**	
	Center atom	energies (cm^{-1})	Center atom	energies (cm^{-1})	Center atom	energies (cm^{-1})
One charge	Dy(1)	884.0	Dy(1)	906.8	Dy(1)	1217
Half charge	Dy(1)	205.4	Dy(1)	223.3	Dy(1)	509.4
Deviation angle (°)		1.082		0.885		4.497

9. References

1. a) D. Casanova, P. Alemany, J. M. Bofill and S. Alvarez, *Chem. Eur. J.*, 2003, **9**, 1281-1295; b) S. Alvarez and M. Llunell, *J. Chem. Soc., Dalton Trans.*, 2000, 3288-3303.
2. D. Reta and N. F. Chilton, *PCCP*, 2019, **21**, 23567-23575.
3. N. F. Chilton, D. Collison, E. J. L. McInnes, R. E. P. Winpenny and A. Soncini, *Nat. Commun.*, 2013, **4**, 2551.